J. Chem. Sci. Vol. 128, No. 4, April 2016, pp. 663–670. © Indian Academy of Sciences.
DOI 10.1007/s12039-016-1041-0

Preparation, characterization and photocatalytic studies of Cu^{2+}, Sn^{2+} and N^{3-} substituted $K_5Sb_5P_2O_{20}$

CH SUDHAKAR REDDY[a], SREENU K[a], J R REDDY[a], A HARI PADMASRI[b], RAVI GUNDEBOINA[a] and M VITHAL[a,*]

[a]Department of Chemistry, Osmania University, Hyderabad 500 007, India
[b]Department of Chemistry, University College for Women, Koti, Osmania University, Hyderabad 500 095, India
e-mail: muga_vithal@osmania.ac.in; muga_vithal@rediffmail.com

MS received 30 November 2015; accepted 8 January 2016

Abstract. Potassium antimony phosphates (K-Sb-P-O) exhibit different structural networks and therefore they were studied as photocatalysts in the present investigation. $K_5Sb_5P_2O_{20}$ was prepared by solid state method. Metal ions (Cu^{2+} and Sn^{2+}), and non-metal anion, N^{3-}, were substituted into the $K_5Sb_5P_2O_{20}$ for possible enhancement of photocatalytic activity. The precursor and substituted compounds were characterized by powder X-ray diffraction, FT-IR, SEM-EDS and UV-Vis diffuse reflectance spectra. Nitrogen substitution into $K_5Sb_5P_2O_{20}$ lattice was studied by O-N-H and XPS measurements. The photocatalytic activity of all the compounds was studied by degradation of methylene blue and methyl violet. The ion-substituted $K_5Sb_5P_2O_{20}$ have shown higher photocatalytic activity against both the dyes. The role of reactive intermediate species produced in the photocatalytic reaction was studied using their appropriate scavengers.

Keywords. Potassium antimony phosphates; visible light; bandgap; photodegradation; OH radicals.

1. Introduction

Phosphates containing alkali, p- and d-block metal (M) ions have been the subject of investigations due to their structural diversity and potential applications. In these materials, the basic building blocks, tetrahedral PO_4 and octahedral MO_6, arrange in different ways to form one-dimensional (1D), two-dimensional (2D) and three-dimensional (3D) structural networks. Piffard *et al.,* reported the synthesis and characterization of a series of potassium antimony phosphates, hereafter abbreviated as K-Sb-P-O, with different dimensionality and a few of them have shown good ionic conductivity.[1–4] It is noticed that the variations in structures from 3D framework to 1D chain depend on the M/P ratio. The alkali metal ions present in the channels (tunnels) can be exchanged with iso/alio-valent ions or sometimes with large organic molecules.[5,6] Among these K-Sb-P-O systems, $K_5Sb_{5-x}Nb_xP_2O_{20}$ has shown a conductivity of $\sim 10^{-3}$ ohm^{-1} cm^{-1} at 500°C which is attributed its skeleton structure with interconnected tunnels that facilitate the movement of alkali ions.[7–10] Phosphates are also considered as good matrices for storage of nuclear wastes (radioactive Cesium) and host for lasing ions.

In addition, metal phosphates have potential applications in the field of catalysis.[11] However, photocatalytic studies of these materials are surprisingly meagre. It is observed that in a few K-Sb-P-O systems, potassium ions can be easily exchanged with iso or aliovalent ions. Based on these strategies, the synthesis of $K_5Sb_5P_2O_{20}$ and exchange of its potassium with copper and tin ions were planned. We have also planned to substitute nitrogen in place of oxygen for higher catalytic activity. The present investigation deals with the preparation of Cu^{2+}, Sn^{2+} and N^{3-} substituted $K_5Sb_5P_2O_{20}$ and their photocatalytic studies against the degradation of methylene blue and methyl violet.

2. Experimental

2.1 *Preparation of $K_5Sb_5P_2O_{20}$(KSPO)*

The precursor material, $K_5Sb_5P_2O_{20}$, was prepared by conventional solid state reaction.[4] KNO_3, Sb_2O_3 and $(NH_4)_2HPO_4$ (all sourced from S D Fine-Chem Limited) were used as starting materials as received. In a typical synthetic process, stoichiometric amounts of KNO_3, Sb_2O_3 and $(NH_4)_2HPO_4$ were ground in an agate mortar for one hour followed by heating at 300°C for 4 h and 1000°C for 24 h with intermittent grinding. A white powder was obtained and designated as KSPO.

*For correspondence

2.2 *Preparation of Cu- and Sn-substituted KSPO (CSPO and SSPO)*

The Cu^{2+} and Sn^{2+} substituted KSPO were prepared by the ion-exchange method. About 0.5 g of KSPO (0.42 mmol) was added to 100 mL each of $CuCl_2$ (2.10 mmol) (for CSPO) and acidified $SnCl_2$ (1.26 mmol) (for SSPO) solutions, separately. Both these solutions were stirred for 24 h at room temperature to ensure complete ion exchange. The resultant solutions were filtered, washed with distilled water and dried in air. The color of the resultant materials was found to be light green and light yellow for CSPO and SSPO, respectively.

2.3 *Preparation of N-substituted KSPO (KSPON)*

Nitrogen substituted KSPO was prepared by heating a mixture of precursor KSPO and urea at 400°C for 2 h in a muffle furnace. The weight ratio of KSPO to urea was 1:2. After the reaction, the product was washed with distilled water and dried in air at 100°C.

2.4 *Characterization*

The room temperature X-ray diffractograms of all samples were recorded using Rigaku MiniFlex 600 X-ray diffractometer (Cu Kα, $\lambda = 1.5406$ Å, $2\theta = 10$–$80°$, step size $(2\theta) = 0.02°$ and scan step time = 0.15 s) for phase confirmation. FT-IR spectra were recorded using Shimadzu spectrometer in the form of KBr pellets. The SEM-EDS images were recorded on the HITACHI SU-1500 variable pressure scanning electron microscope (VP-SEM). JASCO V-650 UV-Vis spectrophotometer was used for UV-Vis diffuse reflectance spectra measurements in the range 200–900 nm. $BaSO_4$ was used as the reflectance standard. O-N-H (Oxygen-nitrogen-hydrogen) analysis was carried out using LECO O-N-H 836 analyzer. The X-ray photoelectron spectroscopic (XPS) measurements were performed on a KRATOS AXIS165 X-ray photoelectron spectrometer using excitation energy of 1253.6 eV (Mg Kα) and pass energy of 80 eV.

2.5 *Photocatalytic experiments*

The photocatalytic activity of all the samples was evaluated by photodegradation of methylene blue (MB) and methyl violet (MV) using HEBER Visible Annular Type Photo-reactor, model HVAR1234 (Haber Scientific, India), under visible light irradiation using 300 W Tungsten lamp as the light source. In a typical process, 50 mL of aqueous MB solution (initial concentration, $C_0 = 1.0\times 10^{-5}$ mol/L) and MV solution ($C_0 = 1.0\times 10^{-5}$ mol/L) was stirred with 0.05 g of catalyst separately in a cylindrical-shaped glass reactor at room temperature in air. The suspension is stirred in the dark for an hour to establish adsorption-desorption equilibrium. Then the solution was exposed to light with continuous stirring. At regular 30 min intervals, about 3 mL of solution was collected and centrifuged to remove the catalyst particles. The change in the concentration of MB was obtained by recording the absorbance at 664 nm using a UV-Vis spectrophotometer. Similar experiments were repeated by using scavengers (Isopropanol, Ammonium oxalate and Benzoquinone) for testing the presence of oxidative species. The reaction mixture consisted of 3 mL of 2 mM scavenger, 47 mL of MB (or MV) and 0.05 g of catalyst.

3. Results and Discussion

KSPO and N-substituted KSPO were prepared by solid state method while the ion-exchange method was adopted for the preparation of Cu- and Sn-substituted KSPO. All the prepared materials were subjected to powder X-ray diffraction (XRD) for phase characterization. The powder XRD patterns of KSPO, CSPO, SSPO and KSPON are shown in figure 1. The d-lines of KSPO are in agreement with the reported data,[4] and free from impurities (JCPDF number: 84-1115). The peak intensities and positions of XRD patterns of the CSPO, SSPO and KSPON vary significantly from that of precursor KSPO. The dissimilarity in the peak intensities and position of d-lines can be expected for ion substituted materials. Theoretically, substitution of other atoms into a lattice will lead to both peak shift and change in intensity. The peak shift occurs because of the difference in size of the substituted ions. The change in intensity of d-lines results from the difference in the electron density of the substituted and host ions. The d-lines of all the samples are refined using POWD software to estimate the cell parameters. It is found that all the samples were crystallized in the orthorhombic lattice with space group Pnnm(58). All the d-lines are indexed and shown in figure 1. The refined cell parameters of all the samples (table S1 in Supplementary Information) and the d-values of KSPO, KSPON, SSPO, and CSPO (in tables S2, S3, S4 and S5, respectively) are given in supporting information. From the refinement of d-values it is observed that d-values of CSPO and SSPO are slightly lower, whereas d-values of KSPON are slightly higher compared to that of the precursor sample. The obtained d-values are in concord with the ionic radius of substituted ions.[12–14] The ionic radius of

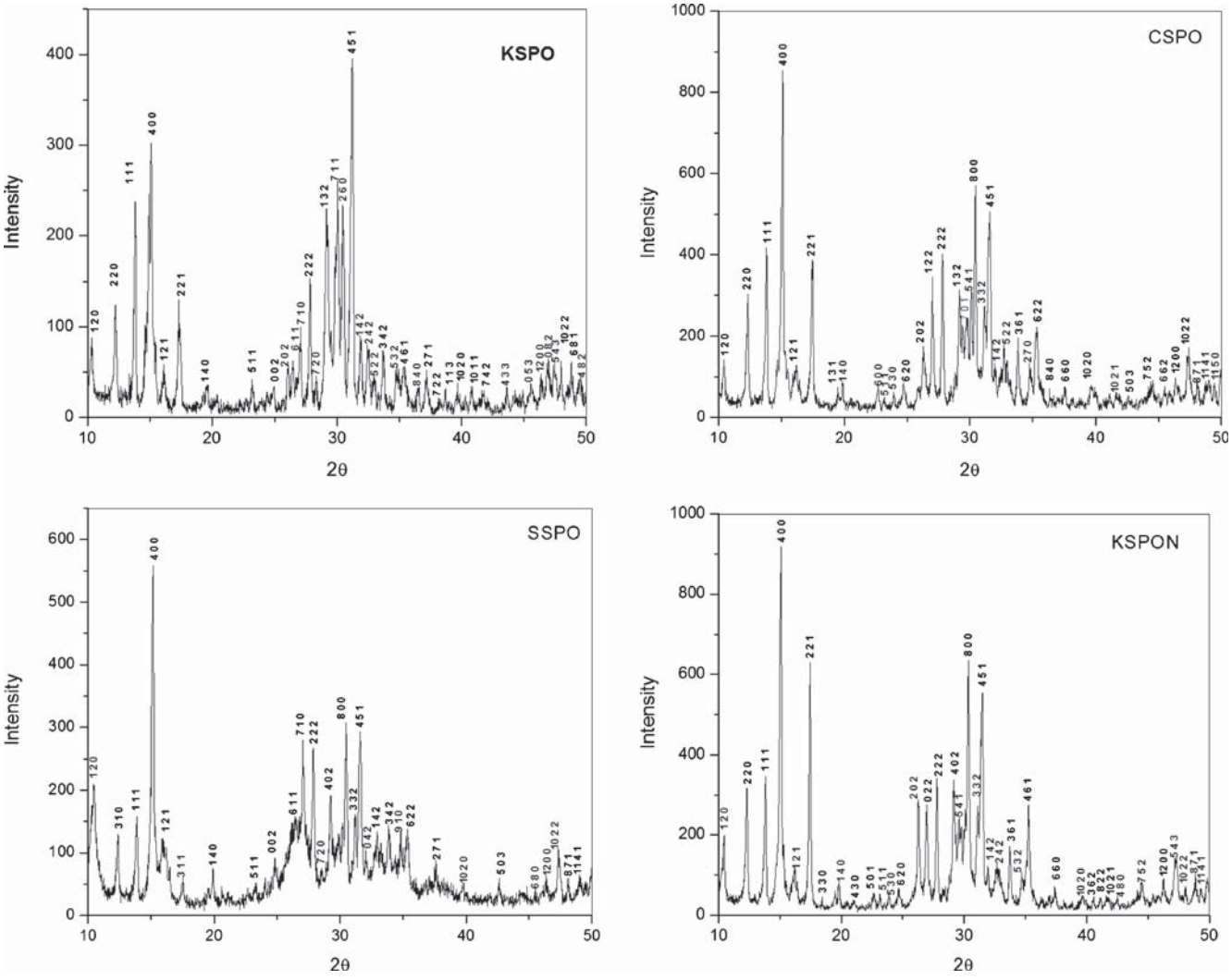

Figure 1. Powder X-ray diffraction patterns of KSPO, CSPO, SSPO and KSPON.

Cu^{2+} (0.73 Å) and Sn^{2+} (1.27 Å) is smaller than the ionic radius of K^+ (1.51 Å), and hence lower d-values are observed in CSPO and SSPO. Similarly, the ionic radius of nitrogen (N^{3-}) (1.71 Å) is higher than the ionic radius of oxygen (O^{2-}) (1.40 Å), and therefore higher d-values are noticed in KSPON.

FT-IR spectra of all the compounds were recorded in the 4000–250 cm^{-1} range to study the vibrational modes of phosphate and antimonite skeletons. All the compositions have exhibited bands below 2000 cm^{-1}. Figure S1 (in Supplementary Information) shows the FT-IR spectra of KSPO, CSPO, SSPO and KSPON in the range 1200–250 cm^{-1}. The IR spectra of the precursor and substituted compounds are similar to each other and akin with the earlier report.[15] The structure of KSPO is constructed by PO_4 and SbO_6 units. Two types of P-O bonds (i.e., terminal P-O bond and bridging P-O bond) and three types of Sb-O bonds (i.e., Sb-O_{cyc}, Sb-O-Sb and Sb-O-P) are found in the KSPO system. The IR spectra of K-Sb-P-O systems were characterized by vibrations corresponding to tetrahedral PO_4 and octahedral SbO_6 polyhedra. The bands in the 900-1300 cm^{-1} region correspond to stretching modes of the PO_4 group.[15] The bands observed in the regions 750-880 cm^{-1}, 670-790 cm^{-1} and 470-680 cm^{-1} can be assigned to the Sb-O_{cyc}, Sb-O-Sb and Sb-O-P stretching vibration modes, respectively.[15] The vibrational positions of all the compounds are given in table S6 (in SI), along with the values reported for $K_5Sb_5P_2O_{20}$.

The optical properties of all the samples were studied from their UV-Vis diffuse reflectance spectra. Figure 2 shows the UV-Vis diffuse reflectance spectra (DRS) of precursor and ion substituted KSPO. The DRS profiles of KSPO, KSPON and SSPO were characterized by a flat portion parallel to the x-axis in the 900-500 nm region followed by steeply rising profiles in the region 500-200 nm. The DRS of CSPO shows, (a) considerable absorption in the region 900–600 nm which can

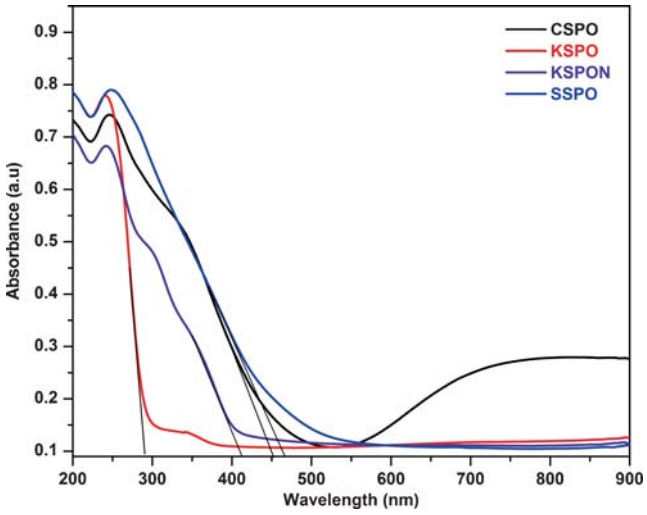

Figure 2. UV-Vis diffuse reflectance spectra of KSPO, CSPO, SSPO and KSPON.

be attributed to weak d-d transitions of octahedral Cu^{2+} ($3d^9$) ions and, (b) a steeply rising portion in the 500-200 nm region. The DRS of KSPO, CSPO, SSPO and KSPON show absorption edges at 290, 451, 465 and 410 nm, respectively. The red shift observed for CSPO, SSPO and KSPON may be due to the mixing of Cu 3d, Sn 5s and N 2p orbitals with valence band O 2p orbitals, which form (Cu 3d + O 2p), (Sn 5s + O 2p) and (N 2p + O 2p) hybrid orbitals, respectively.[16–18] The bandgap energies were calculated as 4.27 (KSPO), 2.74 (CSPO) and 2.66 (SSPO) and 3.02 eV (KSPON) from the equation, $E_g = 1240/\lambda$,[19] where E_g is the band gap energy and λ is the wavelength in nm of the absorption edge.

The morphological studies and elemental analysis were performed for all the samples. Figure 3 shows the SEM photographs of KSPO, CSPO, SSPO and KSPON. The morphology of KSPO shows the segregation of lumps dominated by rod-like objects. The SEM image of CSPO shows clusters with a rod-like and irregular shape of almost equal proportion. The SEM images of SSPO and KSPON show lumps consisting of spherical objects. The elemental composition for KSPO was verified by energy dispersive spectra (figure 4). The EDS profile of KSPO shows the peaks for potassium (K): antimony (Sb): phosphorous (P) in the atomic percent ratio of $\approx$ 20:19:7, respectively, which is comparable with the chemical formula of $K_5Sb_5P_2O_{20}$. In addition, the appearance of Cu, Sn and N peaks in the EDS profiles of CSPO, SSPO and KSPON respectively, suggests that the precursor material was successfully substituted with Cu, Sn and N ions.

The weight percentage of nitrogen was measured quantitatively by O-N-H analysis. The weight percentage of nitrogen was found to be 10.25. The presence

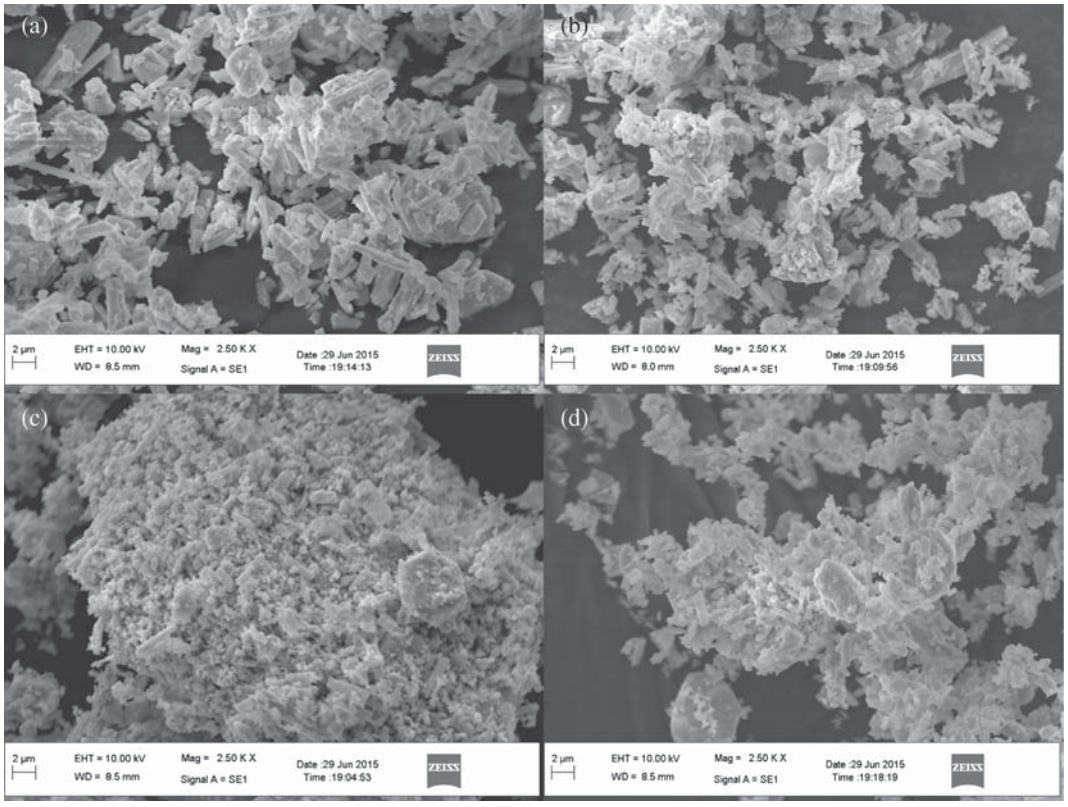

Figure 3. SEM images of (a) KSPO, (b) CSPO, (c) SSPO and (d) KSPON.

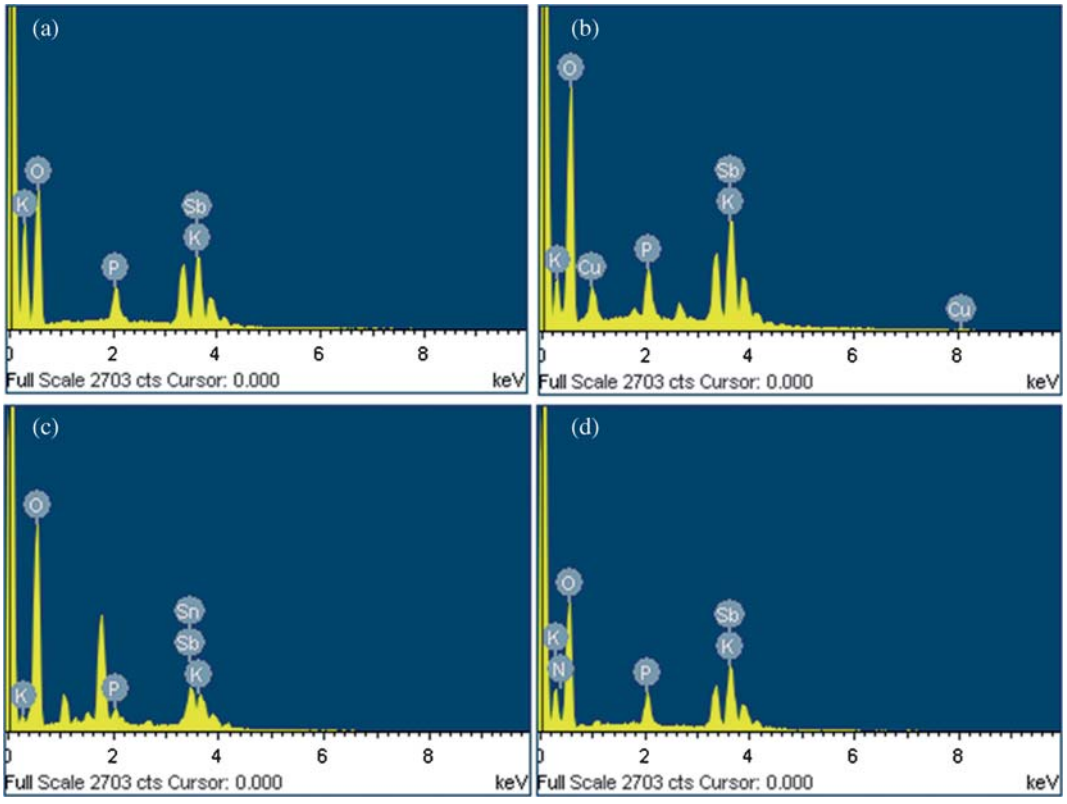

Figure 4. EDS profiles of (a) KSPO, (b) CSPO, (c) SSPO and (d) KSPON.

of nitrogen in KSPON was further substantiated by its XPS analysis. The XPS spectra of KSPO and KSPON are given in supporting information as figures S2 and S3 respectively. The spectra exhibit K, Sb, P and O characteristic peaks along with C 1s peak. The C 1s peak appears due to the contamination of hydrocarbons from the air. Figure S2 shows the surface high resolution XPS spectrum of KSPO. It is characterized by K 2p, Sb 3d, Sb 4d, Sb 4s, P 2p and O 1s profiles. The surface high resolution XPS spectrum of KSPON is shown in figure S3. It is characterized by K 2p, Sb 3d, Sb 4d, Sb 4s, P 2p, N 1s and O 1s profiles. It should be noted that the presence of N 1s peak in KSPON confirms the N doping into KSPO lattice. The binding energy of the N 1s is found to be in the range 394-408 eV depending on the environment of substituted site.[20–22]

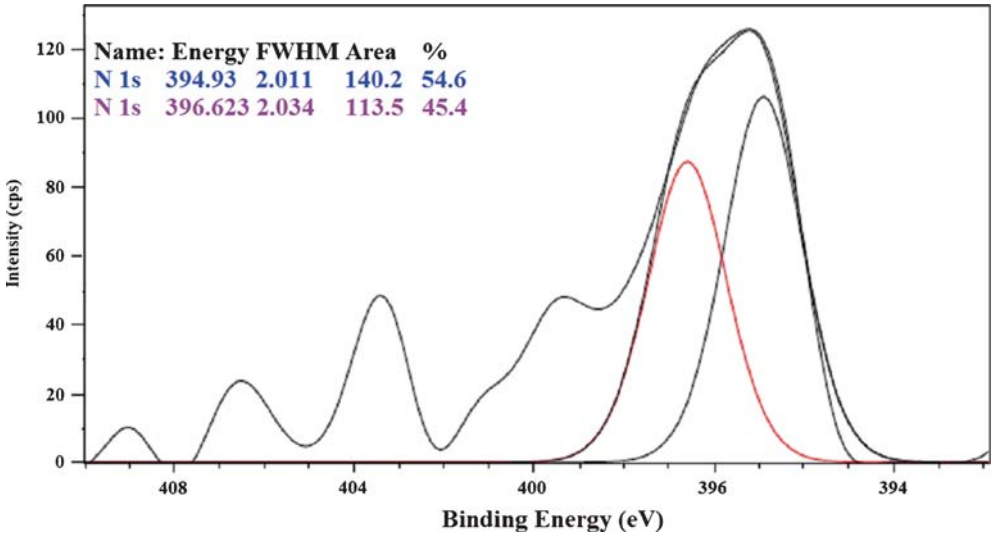

Figure 5. N 1s XPS of KSPON.

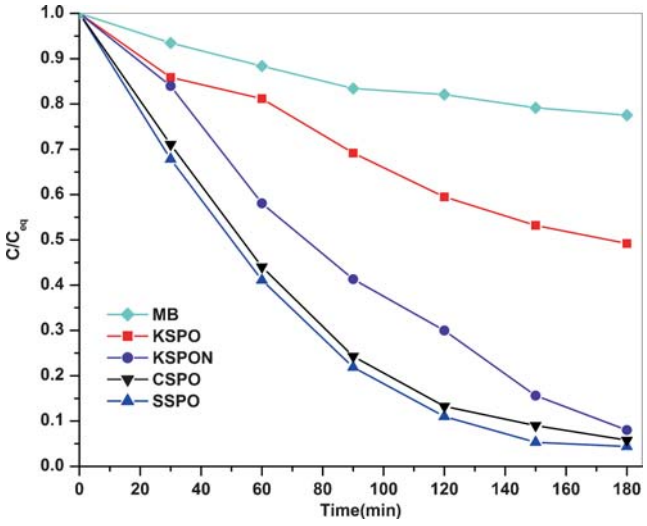

Figure 6. Photocatalytic degradation of MB under visible light irradiation using KSPO, CSPO, SSPO and KSPON.

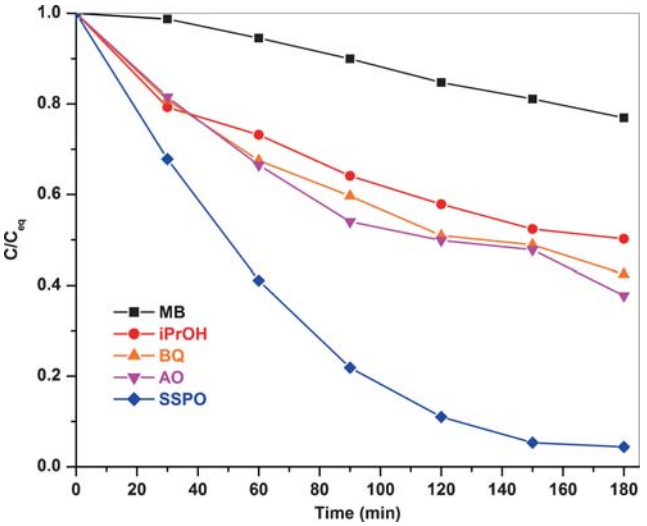

Figure 8. Photodegradation of MB over SSPO in the presence of scavengers.

In the present investigation, the broad N 1s XPS peak observed at 395.5 eV (figure 5) can be deconvoluted into two peaks, at 394.93 and 396.62 eV, and assigned to N 1s in different chemical environments.

Degradation of organic dyes, MB and MV, was done by photocatalysis using KSPO, CSPO, SSPO and KSPON under visible light. The dark experiments were carried out to analyze the extent of adsorbed dye over the catalyst surface. Degradation experiments without catalyst were also performed to estimate the extent of photolysis (decomposition of dye molecules in the presence of light and absence of catalyst). Figure 6 shows the photocatalytic performance of precursor and substituted compounds against photodegradation of MB. In the absence of the catalyst, MB undergoes photolysis to the extent of $\approx$ 23% in 180 min. of visible light irradiation. In figure 6 it is observed that pristine KSPO and ion substituted (CSPO, SSPO and KSPON) KSPO have shown considerable degradation of MB under visible light. However, the degradation of MB in the presence of ion substituted KSPO is more than 90%. The MB degradation in the presence of KSPO, CSPO, SSPO and KSPON is 51, 94, 96 and 92% respectively. The ion substituted KSPO materials show better photocatalytic activity compared to KSPO (figure 6). The higher photoactivity of substituted KSPO could be due to better charge transfer between catalyst and dye molecule preventing any recombination.

Figure 7 shows the photocatalytic degradation of aqueous MV solution in the presence of KSPO, CSPO,

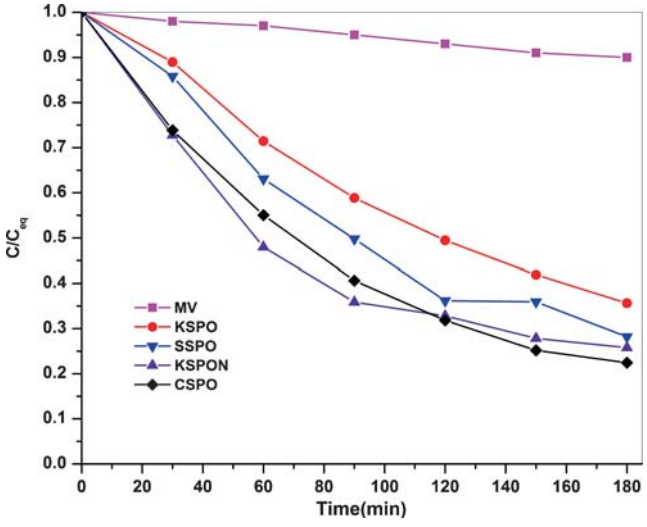

Figure 7. Photocatalytic degradation of MV under visible light irradiation using KSPO, CSPO, SSPO and KSPON.

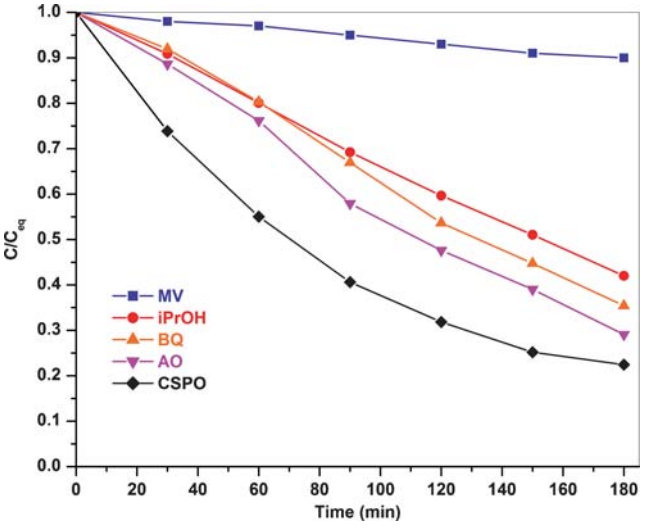

Figure 9. Photodegradation of MV over CSPO in the presence of scavengers.

SSPO and KSPON. The photolysis of MV in 180 min. of visible light irradiation is ≈ 10%. In the case of MV photodegradation also, the substituted compounds have exhibited higher activity compared to precursor KSPO. The extent of degradation of MV after 180 min. of irradiation was found to be 65, 78, 72 and 75% for KSPO, CSPO, SSPO and KSPON respectively. The extent of degradation of MV in the presence of ion substituted KSPO, however, is slightly lower (≈ 70-80%) than the degradation of MB (≈ 90-95%) by the same catalysts under identical experimental conditions.

It is well-known that reactive species such as $^{\bullet}OH$, $^{\bullet}O_2^-$ and h^+ are responsible for the degradation of organic dyes under visible light.[17,23,24] In the present investigation, scavenger experiments were performed to identify the reactive species. Generally, isopropanol (iPrOH), ammonium oxalate (AO) and benzoquinone (BQ) are used as quenchers for $^{\bullet}OH$, h^+ and $^{\bullet}O_2^-$, respectively.[14,25,26] Figure 8 shows the photodegradation of MB over SSPO in the presence and absence of quenchers. From the figure 8, we can observe that the degradation of MB in the presence of hydroxyl radical quencher, iPrOH, is about 50% compared to 96% degradation in the absence of iPrOH. This clearly shows the participation of hydroxyl radicals in the decomposition of MB. Further, if hydroxyl radicals are the only reactive species responsible for the degradation of MB, then the degradation of MB should have been only 20%, a result that equals to photolysis of MB. But the degradation of MB in the presence of iPrOH is 50%. Thus it can be concluded that in addition to hydroxyl radicals, $^{\bullet}O_2^-$ and h^+ are also participating the degradation of MB. Similar results were obtained for the degradation of MB for the catalyst SSPO in the presence of AO and BQ. Scavenger experiments were performed for the degradation of MV using CSPO catalyst also (figure 9). Similar trends were observed in the degradation of MV.

From the above results the photocatalytic mechanism is given as shown below

$$Catalyst\,(KSPO/CSPO/SSPO/KSPON) + h\nu \rightarrow e_{cb}^- + h_{vb}^+ \quad (i)$$

$$H_2O + h_{vb}^+ \rightarrow {}^{\bullet}OH + H^+ \quad (ii)$$

$$O_2 + e_{cb}^- \rightarrow O_2^{\bullet -} \quad (iii)$$

$$O_2^{\bullet -} + H^+ \rightarrow HO_2^{\bullet} \quad (iv)$$

$$2HO_2^{\bullet} \rightarrow H_2O_2 + O_2 \quad (v)$$

$$H_2O_2 \rightarrow 2OH^{\bullet} \quad (vi)$$

$$^{\bullet}OH,\ O_2^{\bullet -},\ h_{vb}^+ + Dye\ (MB/MV) \rightarrow Byproducts \quad (vii)$$

The reusability and cost of the catalysts are important aspects of photocatalysis for practical applications. In order to evaluate the reusability of the catalyst, SSPO (CSPO) was used to degrade MB (MV) in a cyclic manner. The catalyst, SSPO (CSPO), was added into

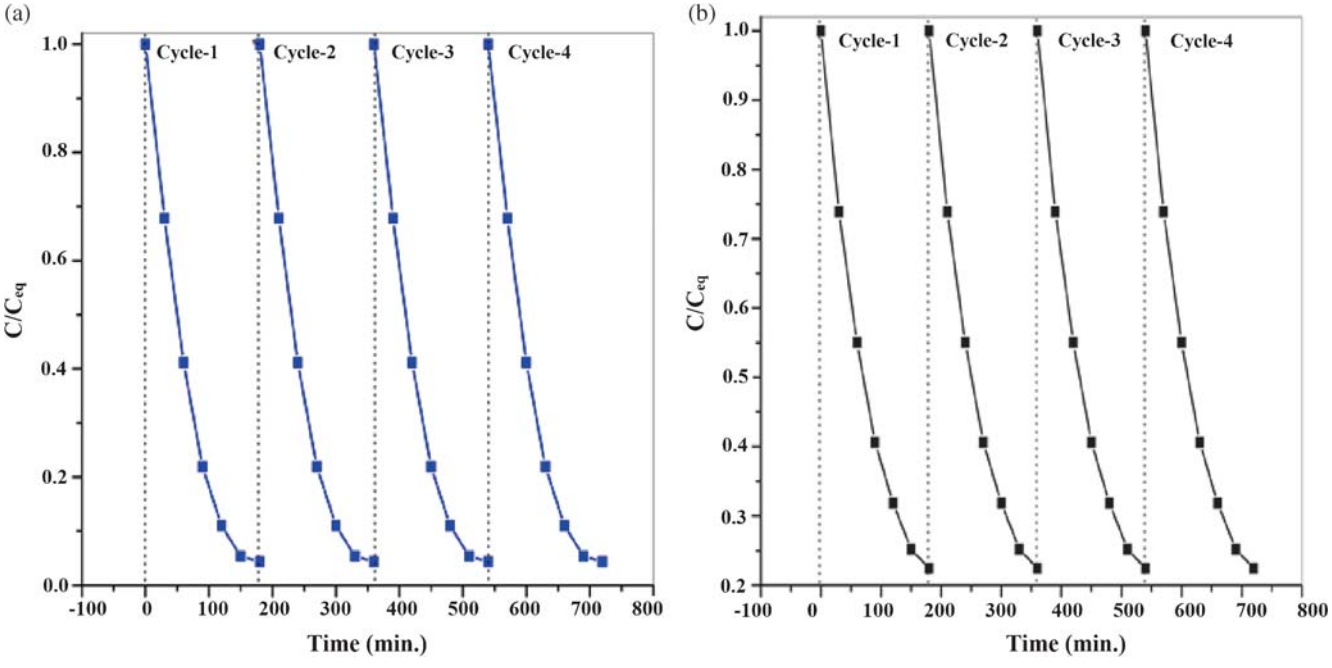

Figure 10. Cyclic runs of (a) SSPO for MB degradation and (b) CSPO for MV degradation.

MB (MV) solution and irradiated with visible light. After 180 min of irradiation, the catalyst was separated, washed with distilled water and dried at room temperature. The same catalyst was used in the second cycle. This process was repeated four times. Figure 10 (a, b) shows the results of reusability of SSPO and CSPO. It is clear from this figure that SSPO and CSPO exhibited the same photoactivity after the fourth cycle also. Thus the catalysts have the potentiality to degrade the organic dyes repeatedly.

4. Conclusions

Potassium antimony phosphate, $K_5Sb_5P_2O_{20}$ (KSPO), has been prepared by solid state method. The ion substituted analogues such as CSPO and SSPO were synthesized by ion exchange method. The nitrogen substituted KSPO was obtained by solid state method. Powder X-ray diffraction patterns of precursor and its ion substituted analogues confirm their phase formation The bandgap energy of the substituted materials was reduced considerably compared to the precursor material. The weight percentage of nitrogen was found to be 10.25 in KSPON. The peaks at 394.93 and 396.62 eV in the deconvoluted XPS of KSPON are assigned to the N 1s in different chemical environments All the compounds have shown significant photocatalytic activity against the degradation of both MB and MV. The ion substituted compounds have exhibited higher activity compared to the precursor oxide. The $^{\bullet}OH$ radicals produced in the photocatalytic reaction play the dominant role in the degradation of organic dyes.

Supplementary Information (SI)

Figures S1 to S3 and tables S1 to S6 are available in electronic Supplementary Information available at http://www.ias.ac.in/Journals/Journal_of_Chemical_Sciences/.

Acknowledgements

Authors would like to thank Department of Science & Technology (DST), New Delhi under FIST scheme and UGC, New Delhi under UPE programme.

References

1. Piffard Y Lachgar A and Tournoux M 1985 *Mater. Res. Bull.* **20** 715
2. Piffard Y, Lachgar A and Tournoux M 1985 *J. Solid State Chem.* **58** 253
3. Piffard Y, Oyetola S, Courant S and Lachgar A 1985 *J. Solid State Chem.* **60** 209
4. Piffard Y, Lachgar A and Tournoux M 1986 *Mater. Res. Bull.* **21** 1231
5. Griffith C S, Luca V, Cochrane J and Hanna J V 2008 *Micropor. Mesopor. Mat.* **111** 387
6. Decaillon J G, Andres Y, Abbe J C and Tournoux M 1998 *Solid State Ionics* **112** 143
7. Wang E and Greenblatt M 1991 *Chem. Mater.* **3** 703
8. Wang B and Greenblatt M 1992 *Chem. Mater.* **4** 657
9. Wang E and Greenblatt M 1991 *Chem. Mater.* **3** 703
10. Wang E and Greenblatt M 1991 *Chem. Mater.* **3** 542
11. Natarajan S and Thomas J M 1992 *Catal. Today* **12** 433
12. Kumar V N, Ravi G, Reddy J R, Suresh P, Muniratnam N R, Prasad G and Vithal M 2014 *J. Am. Ceram. Soc.* **97** 1829
13. Reddy J R, Ravi G, Kumar V N, Radha V Someshwar P, Sreedhar B and Vithal M 2013 *Z. Anorg. Allg. Chem.* **639** 794
14. Reddy J R, Ravinder G, Kumar V N, Shrujana P, Radha V and Vithal M 2015 *J. Alloy Compd.* **618** 815
15. Husson E, Genet F, Lachgar A and Piffard Y 1998 *J. Solid State Chem.* **75** 305
16. Radha V, Ramaswamy K, Ravi G, Munirathnam N R and Vithal M 2015 *Z. Anorg. Allg. Chem.* **641** 935
17. Reddy J R, Kumar V N, Suresh P, Ravi G Ravinder G and Vithal M 2014 *J. Chem. Technol. Biot.* **89** 1833
18. Tong H, Ouyang S, Bi Y, Umezawa N, Oshikiri M and Ye J 2012 *Adv. Mater.* **24** 229
19. He Y, Zhu Y and Wu N 2004 *J. Solid State Chem.* **177** 3868
20. Qiu X and Burda C 2007 *Chem. Phys.* **339** 1
21. Fei Z, Zheng J, Xiaoqin Q, Yongxiang Z, Luyun J, Jinfang Z, Tiancun X and Peter P E 2012 *Chem. Commun.* **48** 8514
22. Yan W, Caixia F, Min Z, Jianjun Y and Zhijun Z 2010 *Appl. Catal. B-Environ.* **100** 84
23. Xiang Q, Yu J and Wong P K 2011 *J. Colloid Interf. Sci.* **357** 163
24. Ishibashi K, Fujishima A, Watanabe T and Hashimoto K 2000 *J. Photoch. Photobio. A* **134** 139
25. Zhang N, Zhang Y, Yang M Q, Tang Z R and Xu Y J 2013 *J. Catal.* **299** 210
26. Xu Y S and Zhang W D 2013 *J. Chem. Soc. Dalton* **42** 1094